

Supplementary Materials

Au₃₆(SePh)₂₄ Nanomolecules: Synthesis, Optical Spectroscopy and Theoretical Analysis

Milan Rambukwella,¹ Le Chang,^{2,3,4} Anish Ravishanker,¹ Luca Sementa,⁴ Alessandro Fortunelli,⁴ Mauro Stener,⁵ Amala Dass^{1,*}

¹ Department of Chemistry and Biochemistry, University of Mississippi, Oxford, Mississippi, 38677, United States

² International Research Center for Soft Matter, Beijing University of Chemical Technology, Beijing 100029, People's Republic of China

³ State Key Laboratory of Organic-Inorganic Composites, Beijing University of Chemical Technology, Beijing 100029, People's Republic of China

⁴ CNR-ICCOM & IPCF, Consiglio Nazionale delle Ricerche, via Giuseppe Moruzzi 1, 56124, Pisa, Italy

⁵ Dipartimento di Scienze Chimiche e Farmaceutiche, Università di Trieste, Trieste I-34127, Italy

Table of content

1. Figure S1. ESI and MALDI mass spectra of Au₃₆(SePh)₂₄ before purification.
2. Figure S2. UV-Vis-NIR spectrum of synthesized Au₃₆(SePh)₂₄.
3. Figure S3. UV-Vis-NIR spectral comparison of Au₃₆(SePh)₂₄ against Au₃₆(SPh)₂₄ and Au₃₆(SPh-tBu)₂₄.
4. Figure S4. Molecular orbital diagrams for Au₃₆(SePh)₂₄ and Au₃₆(SPh)₂₄ nanoclusters.
5. Figure S5. Optical spectrum of Au₃₆(SePh)₂₄ nanocluster distinguished into X, Y and Z components.
6. Figure S6. Optical spectrum of Au₃₆(SPh)₂₄ nanocluster distinguished into X, Y and Z components.
7. Figure S7. ICM-OS plots of X, Y and Z components at 2.0 eV in the optical spectrum of Au₃₆(SePh)₂₄ and Au₃₆(SPh)₂₄ nanoclusters.
8. Figure S8. ICM-OS plots of X, Y and Z components at 2.85 eV in the optical spectrum of Au₃₆(SePh)₂₄ and Au₃₆(SPh)₂₄ nanoclusters.

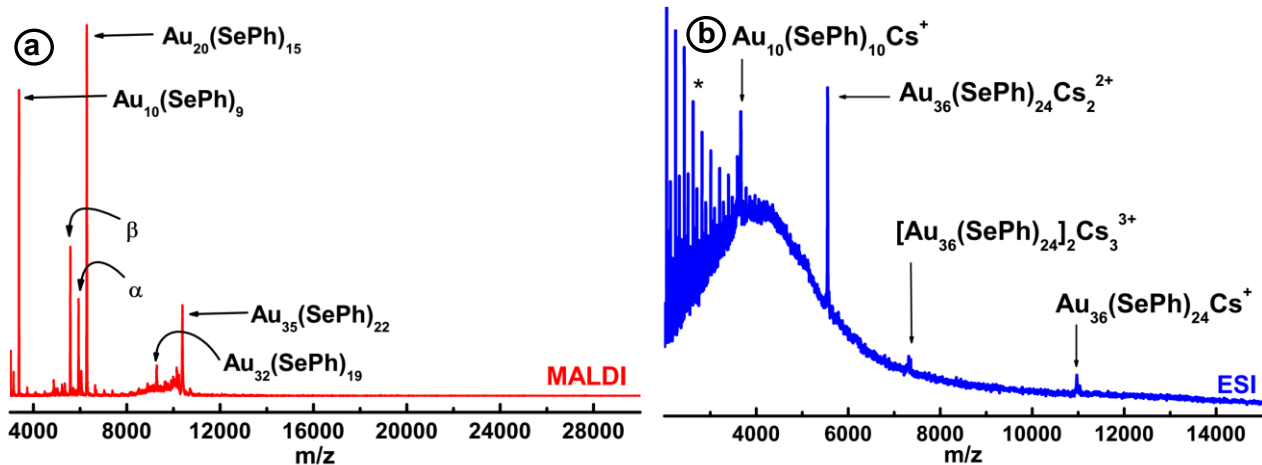


Figure S1. (a) MALDI mass spectra of the as-synthesized product. Intact $\text{Au}_{36}(\text{SePh})_{24}$ species was not observed due to loss of $\text{Au}(\text{SePh})_2$ and instead $\text{Au}_{35}(\text{SePh})_{22}$ fragment was observed. $\text{Au}_{32}(\text{SePh})_{19}$ fragment was observed due to further fragmentation of $\text{Au}_{36}(\text{SePh})_{24}$. In addition to dominant $\text{Au}_{36}(\text{SePh})_{24}$ nanomolecules trace amounts of $\text{Au}_{20}(\text{SePh})_{16}$ and $\text{Au}_{10}(\text{SePh})_{10}$ nanomolecules were observed as by-products of the ligand-exchange reaction. One ligand lost corresponding fragments were observed for each nanomolecule. α and β indicates fragment peaks of $\text{Au}_{20}(\text{SePh})_{16}$ due to successive loss of $\text{Au}(\text{SePh})$ (b) ESI mass spectrum of the as synthesized $\text{Au}_{36}(\text{SePh})_{24}$ nanomolecules before purification. Spectrum shows 1+, 2+ and dimerized 3+ charge species of $\text{Au}_{36}(\text{SePh})_{24}$ nanomolecules. At low mass $\text{Au}_{10}(\text{SePh})_{10}\text{Cs}^+$ was observed and the asterisk shows CsCH_3COO clusters at mass below 5000 m/z .

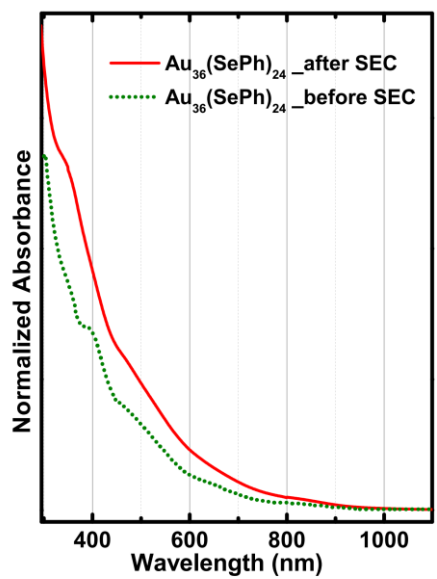


Figure S2. Comparison of UV-Vis-NIR spectra of the $\text{Au}_{36}(\text{SePh})_{24}$ before and after SEC purification. The spectra illustrate that major product of the as synthesized reaction is $\text{Au}_{36}(\text{SePh})_{24}$ nanomolecules.

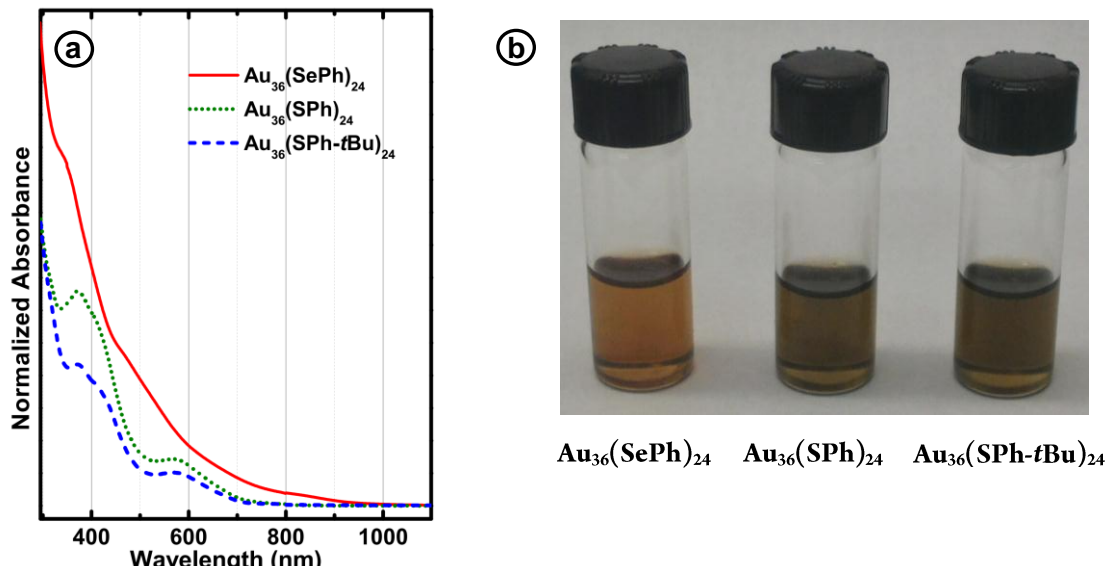


Figure S3. (a) Comparison of UV-Vis-NIR spectra of the $\text{Au}_{36}(\text{SePh})_{24}$ nanomolecules against $\text{Au}_{36}(\text{SPh})_{24}$ and $\text{Au}_{36}(\text{SPh}-t\text{Bu})_{24}$ nanomolecules and (b) visual color comparison of corresponding nanomolecules respectively. $\text{Au}_{36}(\text{SePh})_{24}$ nanomolecules in solution is reddish-brown in color where as $\text{Au}_{36}(\text{SPh})_{24}$ and $\text{Au}_{36}(\text{SPh}-t\text{Bu})_{24}$ are green and does not have a distinct color difference between latter two nanomolecules.

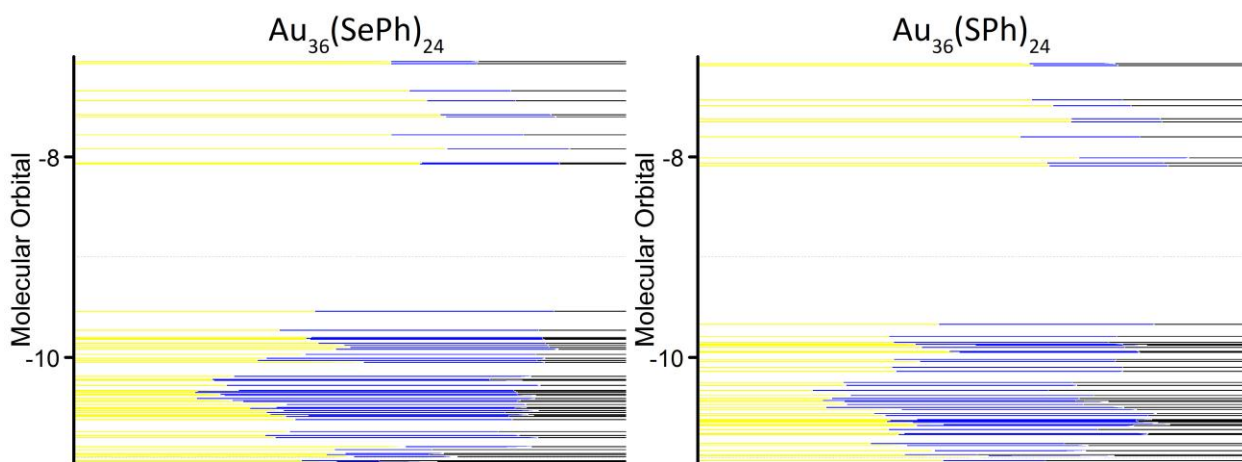


Fig S4 Molecular orbital diagrams for $\text{Au}_{36}(\text{SePh})_{24}$ and $\text{Au}_{36}(\text{SPh})_{24}$ nanoclusters.

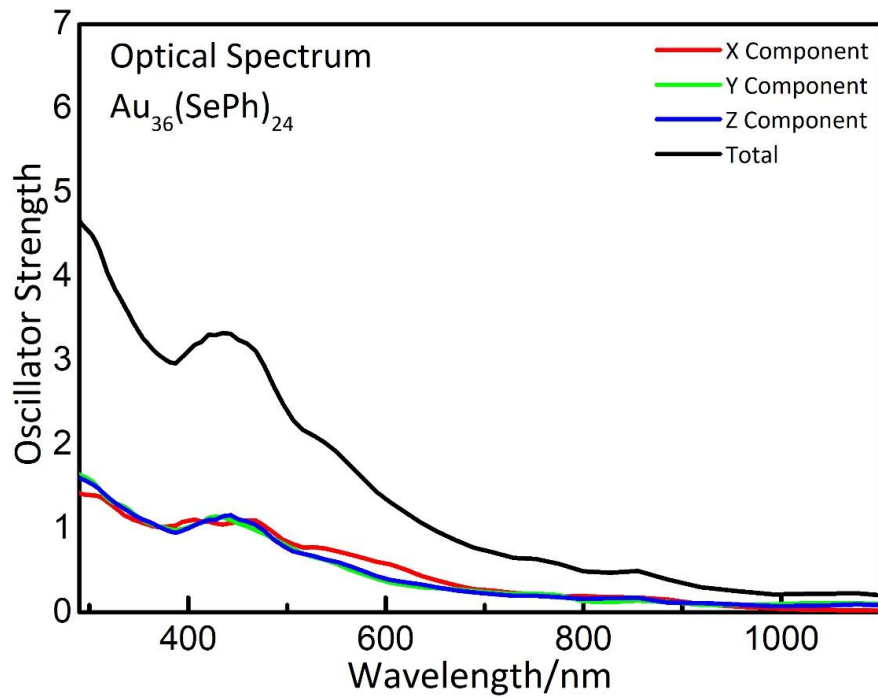


Fig S5 Optical spectrum of $\text{Au}_{36}(\text{SePh})_{24}$ nanocluster distinguished into X, Y and Z components.

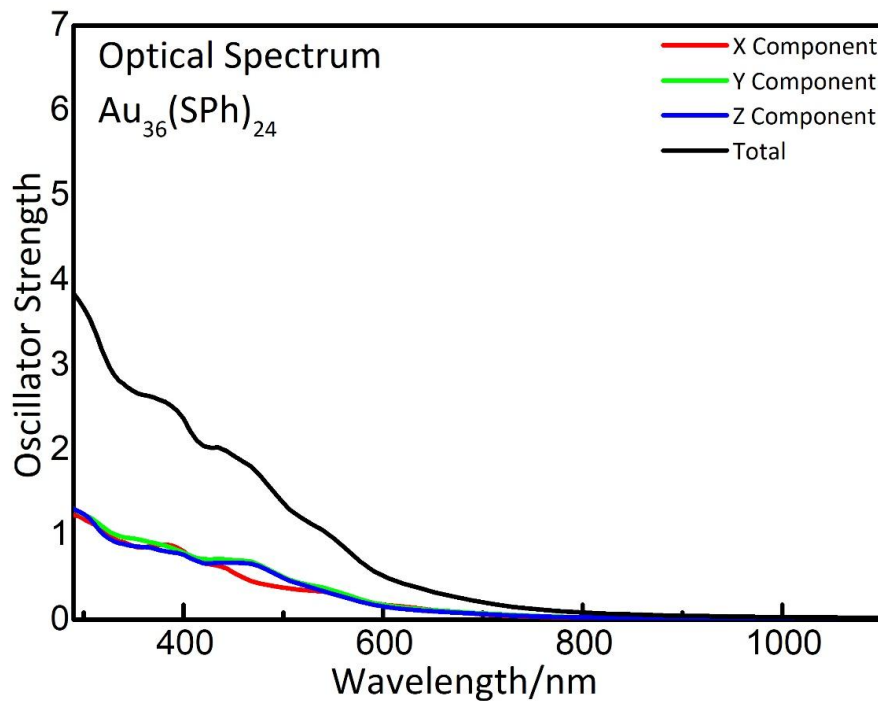
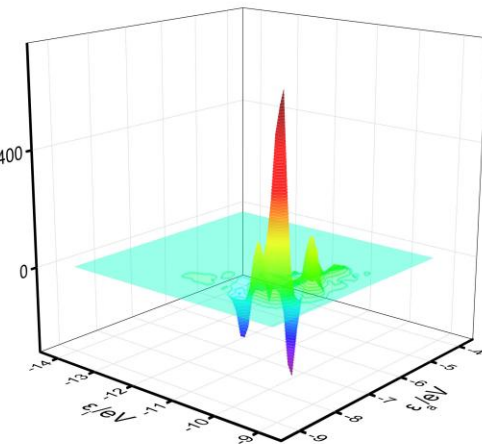


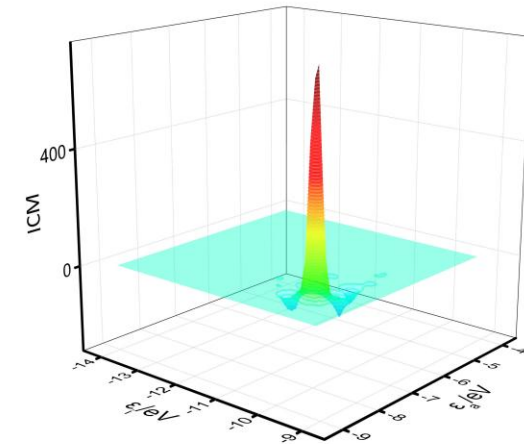
Fig S6 Optical spectrum of $\text{Au}_{36}(\text{SPh})_{24}$ nanocluster distinguished into X, Y and Z components.



2.0X



2.0Y



2.0Z

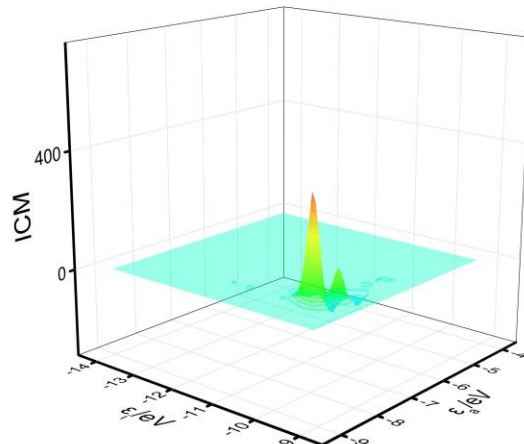


Fig S7 ICM-OS plots of X, Y and Z components at 2.0 eV in the optical spectrum of $\text{Au}_{36}(\text{SePh})_{24}$ and $\text{Au}_{36}(\text{SPh})_{24}$ nanoclusters.

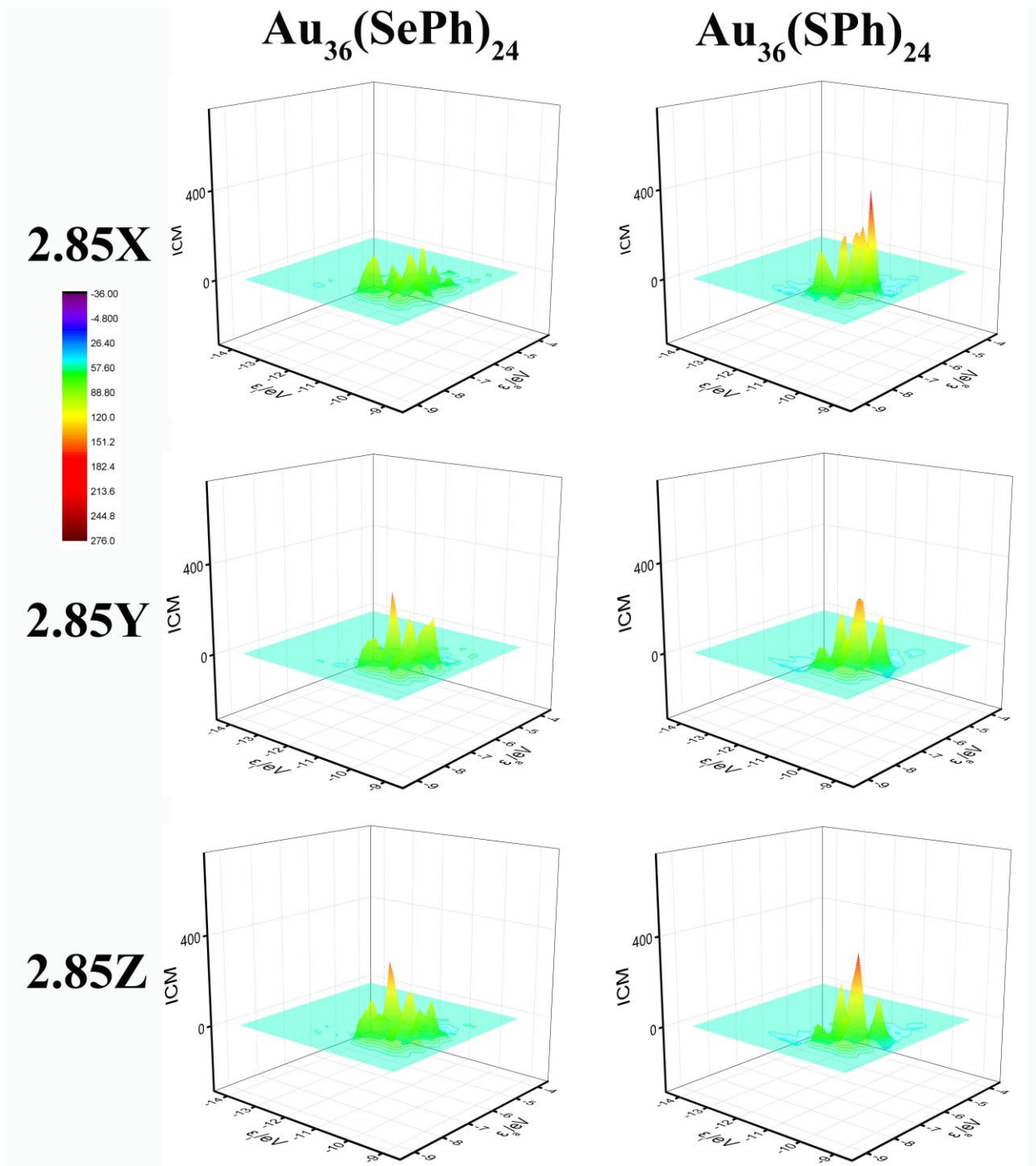


Fig S8 ICM plots of X, Y and Z components at 2.85 eV in the optical spectrum of $\text{Au}_{36}(\text{SePh})_{24}$ and $\text{Au}_{36}(\text{SPh})_{24}$ nanoclusters.

Table S1 Single-particle contributions to oscillator strength at 2.0 eV in the optical spectrum of $\text{Au}_{36}(\text{SePh})_{24}$ and $\text{Au}_{36}(\text{SPh})_{24}$. Contributions are included until 70% of the oscillator strength is obtained.

Au36(SePh) ₂₄					Au36(SPh) ₂₄						
i	j	dipole	C _{ij}	C _{ij} *dipole	%	i	j	dipole	C _{ij}	C _{ij} *dipole	%
H-04	L+02	-1.7487	-0.3348	0.585	8.37	H-04	L+02	-2.2903	-0.3774	0.864	14.99
H-12	L+02	-0.9716	0.2241	-0.218	3.75	H-09	L+02	-0.0344	0.2958	-0.010	9.2
H-10	L+02	0.4140	0.2018	0.084	3.04	H-05	LUMO	-0.8178	-0.2795	0.229	8.22
H-01	L+02	-0.8023	-0.1800	0.144	2.42	H-07	LUMO	-2.0100	-0.2660	0.535	7.44
H-13	L+01	0.0732	0.1800	0.013	2.42	H-08	L+02	-1.2951	-0.2605	0.337	7.14
H-04	L+02	-1.1040	-0.1751	0.193	2.29	H-02	L+01	0.5822	0.2120	0.123	4.73
H-09	L+03	-1.2965	-0.1642	0.213	2.01	H-07	L+01	-1.1082	-0.1968	0.218	4.08
HOMO	L+07	-2.2877	-0.1499	0.343	1.68	H-05	L+01	0.9665	0.1840	0.178	3.56
H-06	LUMO	0.7642	0.1483	0.113	1.64	H-03	L+01	0.3602	0.1620	0.058	2.76
H-02	L+01	-0.8164	-0.1396	0.114	1.45	H-03	L+02	0.7791	0.1599	0.125	2.69
H-03	LUMO	-0.7796	-0.1387	0.108	1.44	H-06	LUMO	-0.9015	-0.1539	0.139	2.49
H-14	L+01	-0.9867	-0.1368	0.135	1.4	H-06	L+01	1.5883	0.1524	0.242	2.44
H-15	LUMO	-0.7201	-0.1332	0.096	1.32						
H-08	L+01	-0.4554	-0.1330	0.061	1.32						
H-03	L+08	-0.5399	-0.1263	0.068	1.19						
H-26	L+01	-0.0888	-0.1204	0.011	1.08						
H-25	LUMO	0.2770	0.1190	0.033	1.06						
H-08	L+02	1.1409	0.1166	0.133	1.01						
H-06	L+05	1.0143	-0.1160	-0.118	1						
H-17	L+01	0.1024	0.1119	0.011	0.94						
H-13	LUMO	0.6244	0.1110	0.069	0.92						
H-02	L+04	-0.7504	0.1090	-0.082	0.89						
H-26	LUMO	0.4371	-0.1064	-0.047	0.85						
H-08	L+06	0.4556	0.1037	0.047	0.8						
H-07	L+02	-0.8183	-0.1024	0.084	0.78						
H-05	L+09	0.6236	0.1007	0.063	0.76						
H-04	L+06	0.1148	0.0991	0.011	0.73						
H-02	L+09	-0.5433	-0.0979	0.053	0.72						
H-05	L+07	0.6907	0.0974	0.067	0.71						
H-02	L+08	-0.5488	-0.0964	0.053	0.69						
H-20	L+01	0.1060	0.0946	0.010	0.67						
H-03	L+02	0.9695	0.0928	0.090	0.64						
H-11	L+01	-0.1999	-0.0918	0.018	0.63						
H-29	LUMO	0.6286	-0.0912	-0.057	0.62						
H-10	L+01	0.1241	0.0905	0.011	0.61						
H-03	L+04	-0.5525	0.0904	-0.050	0.61						
H-30	LUMO	-0.2950	0.0878	-0.026	0.58						
HOMO	L+05	0.5478	0.0851	0.047	0.54						
H-05	LUMO	0.1737	-0.0848	-0.015	0.54						
H-32	L+06	0.2906	-0.0847	-0.025	0.54						
H-04	L+05	-1.3650	0.0833	-0.114	0.52						
H-12	L+01	-0.6501	-0.0831	0.054	0.52						
H-03	L+05	-0.5673	0.0829	-0.047	0.51						
H-07	L+01	-0.8564	-0.0821	0.070	0.5						
H-16	L+02	-0.5836	-0.0818	0.048	0.5						
H-09	LUMO	0.7547	0.0815	0.061	0.5						
H-07	L+04	-0.7517	0.0792	-0.060	0.47						
HOMO	L+06	-0.3217	-0.0788	0.025	0.46						
H-02	L+05	0.2728	-0.0788	-0.021	0.46						
H-05	L+02	-0.8419	-0.0786	0.066	0.46						
H-24	L+06	0.0505	0.0766	0.004	0.44						
H-07	L+06	0.2287	-0.0764	-0.017	0.44						
H-05	L+06	0.1246	0.0759	0.009	0.43						
H-28	LUMO	-0.0951	0.0743	-0.007	0.41						
H-25	L+01	0.8554	-0.0701	-0.060	0.37						
H-32	L+01	-0.3906	0.0693	-0.027	0.36						
H-04	L+09	0.6200	0.0690	0.043	0.36						

H-30	L+01	0.2839	-0.0677	-0.019	0.34
H-07	L+08	0.8302	0.0677	0.056	0.34
H-28	L+01	-0.6621	0.0675	-0.045	0.34
H-06	L+04	-0.6037	0.0661	-0.040	0.33
H-09	L+02	-0.1174	0.0649	-0.008	0.31
H-06	L+01	-1.4693	-0.0648	0.095	0.31
H-17	LUMO	0.0021	-0.0646	0.000	0.31
H-17	L+03	-0.2578	-0.0645	0.017	0.31
H-01	L+03	-0.2789	-0.0641	0.018	0.31
H-13	L+02	-0.0440	0.0638	-0.003	0.3
H-02	L+60	0.0926	-0.0627	-0.006	0.29
H-03	L+01	0.2944	-0.0625	-0.018	0.29
H-29	L+01	0.0774	-0.0625	-0.005	0.29
H-01	LUMO	-0.2493	-0.0622	0.016	0.29
H-11	L+02	0.0293	-0.0620	-0.002	0.29
H-02	L+15	-0.1018	-0.0620	0.006	0.29
H-23	L+03	0.1386	0.0619	0.009	0.29
H-31	L+01	0.4422	-0.0614	-0.027	0.28
H-03	L+06	-0.1487	-0.0606	0.009	0.27
H-04	L+07	-0.0356	-0.0604	0.002	0.27
H-37	L+03	-0.8003	0.0600	-0.048	0.27
H-15	L+01	0.2789	0.0594	0.017	0.26
H-18	L+02	-1.0276	-0.0582	0.060	0.25
H-05	L+08	-0.4433	-0.0578	0.026	0.25
H-14	LUMO	0.0505	0.0570	0.003	0.24

Table S2 Single-particle contributions to oscillator strength at 2.85 eV in the optical spectrum of $\text{Au}_{36}(\text{SePh})_{24}$ and $\text{Au}_{36}(\text{SPh})_{24}$. Contributions are included until 50% of the oscillator strength is obtained.

$\text{Au}_{36}(\text{SePh})_{24}$					$\text{Au}_{36}(\text{SPh})_{24}$						
i	j	dipole	C_{ij}	$C_{ij}^*\text{dipole}$	%	i	j	dipole	C_{ij}	$C_{ij}^*\text{dipole}$	%
H-06	L+08	-0.7057	-0.1452	0.102	2.02	H-05	L+08	-1.1879	-0.2287	0.272	4.59
H-34	L+02	0.5245	0.1358	0.071	1.77	H-02	L+09	-1.2205	-0.2284	0.279	4.58
H-12	L+06	-1.3784	-0.1300	0.179	1.62	H-07	L+08	-0.2650	-0.2212	0.059	4.3
H-01	L+14	-0.5058	-0.1244	0.063	1.48	H-09	L+06	1.4345	0.2104	0.302	3.89
H-06	L+09	0.5492	0.1201	0.066	1.38	H-01	L+06	-2.0432	-0.1918	0.392	3.23
H-08	L+09	0.4945	0.1189	0.059	1.35	H-05	L+09	-0.2891	-0.1837	0.053	2.96
H-24	L+05	-0.2175	-0.1153	0.025	1.27	H-06	L+09	0.0815	-0.1540	-0.013	2.08
H-36	L+02	0.4172	0.1134	0.047	1.23	H-26	L+01	0.6658	0.1520	0.101	2.03
H-04	L+11	-0.0814	0.1087	-0.009	1.13	HOMO	L+07	-2.3307	-0.1426	0.332	1.79
H-18	L+05	-0.3921	-0.1018	0.040	0.99	H-07	L+05	1.0247	0.1405	0.144	1.73
H-38	LUMO	-0.3159	-0.1012	0.032	0.98	H-06	L+04	1.3179	0.1260	0.166	1.39
H-25	L+03	0.2315	0.1010	0.023	0.98	H-02	L+08	0.4412	0.1193	0.053	1.25
H-33	LUMO	0.7719	0.1008	0.078	0.97	H-06	L+08	-0.3965	-0.1151	0.046	1.16
H-07	L+08	0.8302	0.0985	0.082	0.93	H-28	LUMO	-0.4998	-0.1121	0.056	1.1
H-11	L+09	0.1134	0.0968	0.011	0.9	H-19	L+05	0.1807	0.1089	0.020	1.04
H-09	L+09	-0.3957	-0.0949	0.038	0.86	H-12	L+06	-0.6937	-0.1053	0.073	0.97
H-35	L+01	0.3313	0.0949	0.031	0.86	H-03	L+09	-0.3662	-0.0996	0.036	0.87
HOMO	L+31	0.4307	0.0938	0.040	0.84	H-14	L+05	0.3649	0.0980	0.036	0.84
H-07	L+09	0.4314	0.0916	0.040	0.8	H-02	L+11	0.4366	0.0957	0.042	0.8
H-36	L+01	0.5497	0.0912	0.050	0.8	H-04	L+08	-0.3030	-0.0911	0.028	0.73
H-37	LUMO	0.2789	0.0905	0.025	0.78	H-07	L+09	0.6427	0.0903	0.058	0.72
H-01	L+11	-0.3692	-0.0885	0.033	0.75	H-22	L+01	0.4978	0.0885	0.044	0.69
H-17	L+04	-0.2173	-0.0869	0.019	0.72	H-25	LUMO	-0.3991	-0.0883	0.035	0.68
H-01	L+15	0.1815	0.0865	0.016	0.72	H-20	L+05	-0.2854	-0.0863	0.025	0.65
H-39	L+01	0.3638	0.0863	0.031	0.71	H-27	LUMO	-0.3888	-0.0839	0.033	0.62
H-27	L+03	0.1752	0.0811	0.014	0.63	H-04	L+02	-2.2903	-0.0827	0.189	0.6
H-08	L+18	0.0289	-0.0810	-0.002	0.63	H-10	L+06	0.8374	0.0804	0.067	0.57
H-32	L+02	-0.4570	-0.0789	0.036	0.6	H-07	LUMO	-2.0100	-0.0793	0.159	0.55
H-32	L+01	-0.3906	-0.0781	0.031	0.58	H-33	L+06	0.4657	-0.0787	-0.037	0.54
H-01	L+06	1.8929	0.0775	0.147	0.58	H-25	L+02	-0.6743	-0.0761	0.051	0.51
H-22	L+05	0.2394	0.0774	0.019	0.57	H-03	L+11	0.5263	0.0738	0.039	0.48
H-08	L+15	0.0941	0.0768	0.007	0.57	H-37	LUMO	-0.5302	-0.0709	0.038	0.44
H-06	L+05	1.0143	0.0766	0.078	0.56	H-15	L+07	-0.3880	-0.0709	0.027	0.44
H-35	LUMO	0.5461	0.0766	0.042	0.56	H-35	L+01	-0.0837	0.0703	-0.006	0.43
H-13	L+04	-0.2216	-0.0754	0.017	0.54	H-13	L+01	1.5370	0.0688	0.106	0.42
H-29	LUMO	0.6286	0.0740	0.047	0.52	H-14	L+06	0.0543	0.0685	0.004	0.41
H-31	L+01	0.4422	0.0737	0.033	0.52						
H-23	L+05	0.3179	0.0722	0.023	0.5						
H-18	L+06	-0.2342	-0.0719	0.017	0.5						
H-02	L+21	-0.4655	-0.0714	0.033	0.49						
H-28	L+04	0.0680	-0.0696	-0.005	0.46						
HOMO	L+34	0.3658	0.0685	0.025	0.45						
H-01	L+10	-0.1781	0.0662	-0.012	0.42						
H-13	L+06	0.3118	0.0657	0.020	0.41						
H-21	L+05	-0.7562	-0.0657	0.050	0.41						
H-36	LUMO	-0.2476	-0.0648	0.016	0.4						
H-14	L+05	-0.1582	-0.0642	0.010	0.39						
H-19	L+05	0.0372	0.0635	0.002	0.39						
H-06	L+06	0.5875	0.0634	0.037	0.39						
H-17	L+06	0.0884	0.0612	0.005	0.36						
HOMO	L+25	0.2897	0.0610	0.018	0.36						
H-19	L+04	0.5425	0.0596	0.032	0.34						
H-28	L+01	-0.6621	-0.0583	0.039	0.33						
H-10	L+08	-0.1571	0.0581	-0.009	0.32						
H-03	L+08	-0.5399	0.0577	-0.031	0.32						
H-42	L+01	-0.0022	-0.0571	0.000	0.31						
H-01	L+19	0.4099	0.0571	0.023	0.31						

H-07	L+04	-0.7517	-0.0565	0.042	0.31
H-30	LUMO	-0.2950	-0.0564	0.017	0.31
H-28	L+03	0.1357	0.0562	0.008	0.3
H-12	L+15	0.0719	-0.0562	-0.004	0.3
H-41	L+01	-0.0101	0.0555	-0.001	0.29
H-32	LUMO	0.0292	0.0549	0.002	0.29
H-30	L+03	0.2012	0.0548	0.011	0.29
H-02	L+27	-0.0822	0.0535	-0.004	0.27
H-04	L+05	-1.3650	-0.0532	0.073	0.27
H-32	L+03	-0.0455	-0.0519	0.002	0.26
H-29	L+05	0.1905	0.0517	0.010	0.26
H-25	L+04	-0.2131	-0.0511	0.011	0.25
H-26	L+01	-0.0888	0.0503	-0.004	0.24
H-09	L+03	-1.2965	-0.0501	0.065	0.24
H-10	L+06	0.1277	-0.0499	-0.006	0.24
H-31	L+05	-0.1103	-0.0491	0.005	0.23
H-08	L+04	-0.5245	-0.0488	0.026	0.23
HOMO	L+07	-2.2877	-0.0473	0.108	0.21
H-02	L+09	-0.5433	0.0472	-0.026	0.21
H-23	LUMO	0.9433	0.0470	0.044	0.21
H-27	L+06	0.2766	0.0470	0.013	0.21
H-30	L+07	-0.2449	-0.0470	0.012	0.21
H-16	L+06	-0.1921	-0.0469	0.009	0.21
H-12	L+18	-0.1558	0.0468	-0.007	0.21
HOMO	L+29	-0.3001	-0.0466	0.014	0.21
HOMO	L+53	-0.3068	-0.0453	0.014	0.2
H-43	LUMO	-0.0068	0.0450	0.000	0.19
H-34	LUMO	0.1975	0.0446	0.009	0.19
H-12	L+02	-0.9716	-0.0445	0.043	0.19
H-38	L+01	-0.0131	-0.0432	0.001	0.18
H-25	L+01	0.8554	0.0432	0.037	0.18
H-17	L+07	0.0077	-0.0430	0.000	0.18
H-28	L+06	-0.3644	-0.0426	0.016	0.17
H-02	L+18	-0.1089	0.0424	-0.005	0.17
H-01	L+12	-0.1683	-0.0423	0.007	0.17
H-04	L+60	0.2800	0.0419	0.012	0.17
H-02	L+78	0.0282	-0.0418	-0.001	0.17